We P5 16

Low-Frequency Phase Estimation for Broadband Seismic Using Tomography Velocity Models

A. JafarGandomi (CGG), V. Souvannavong (CGG), H. Hoeber* (CGG)

Summary

We present a method to estimate and correct the phase of broadband seismic data in the low-frequency range using the tomography velocity model as an analogy for subsurface geology. The high-resolution velocity model is obtained from travel-time tomography and therefore has minimal influence from seismic amplitude and phase in the low-frequency range. We derive a phase-correction operator by matching between seismic data and zero-phase synthetics that are built based on a realization of reflectivity obtained from the tomographic inversion. We discuss the robustness of the method with synthetic data and show real data examples demonstrating improved well-tie and impedance inversion results.

Introduction

The value of low frequencies for quantitative and qualitative interpretation has been extensively discussed in recent years. However, preserving and controlling the quality of the low frequencies during the seismic processing is challenging. Ideally, we would like the seismic to be zero-phase; in order to proceed with inversion, we certainly need to know the phase of the wavelet at all frequencies.

Residual phase in the processed seismic data can be quantified through statistical (Longbottom et al., 1988; Yang et al.,2016) and deterministic wavelet analysis such as a well-ties. In wavelet estimation from well-ties the seismic is modelled as the convolution of reflectivity and wavelet so that the seismic phase is the sum of locally known "geological phase" and unknown wavelet phase. The reliability of this method is compromised due to the limited spatial and temporal extent of the well-log measurements (Shakel & Mesdag, 2014). Our proposed method also relies on the convolutional model and the separation of geological and wavelet phases. However, by using high-resolution velocity models obtained from travel-time tomography we can remove both uncertainties inherent in well-ties: the tomographic inversion provides continuous coverage spatially and temporally. As we will show, this allows for the accurate estimation of wavelet phase in the overlapping frequency range between broadband seismic and high-resolution tomography models.

Phase of geology and high-resolution velocity models

We describe the data using a noise-free convolutional model,

$$S(\omega) = w(\omega).r(\omega), \quad (1)$$

where *S*, *w*, and *r* are complex variables. Equation 1 may be recast into,

$$A_S(\omega)e^{i\phi_S(\omega)} = A_w(\omega)e^{i\phi_w(\omega)}.A_r(\omega)e^{i\phi_r(\omega)}, \quad (2)$$

where *A*, ϕ, and ω indicate magnitude, phase, and angular frequency, respectively. Subscripts *S*, *r*, and *w* indicate seismic, reflectivity and wavelet, respecively. We need to determine ϕ_w which requires to dis-entangle ϕ_r from ϕ_S.

Figure 1 shows the derivative of the phase ($\partial\phi/\partial f$) with respect to frequency for three dipoles with varying layer-thickness. In a realistic setting, with many different dipoles, statistical wavelet-estimation methods can, in principle, cancel out the geological phase by increasing the size of the estimation window. A smaller estimation window will be sensitive to localized phase anomalies, such as those in Figure 1, which are due to geological effects (Edgar & Selvage, 2011). However, Figure 1 shows that there is less phase sensitivity and variability in the lower-frequency range, which makes statistical cancellation more difficult. In such situations the wavelet estimation must be constrained with a priori geological information. Recent developments in travel-time tomography provide reliable estimates of subsurface geology up to 6-8 Hz (e.g., Vigée et al., 2014). Furthermore, the lower bound

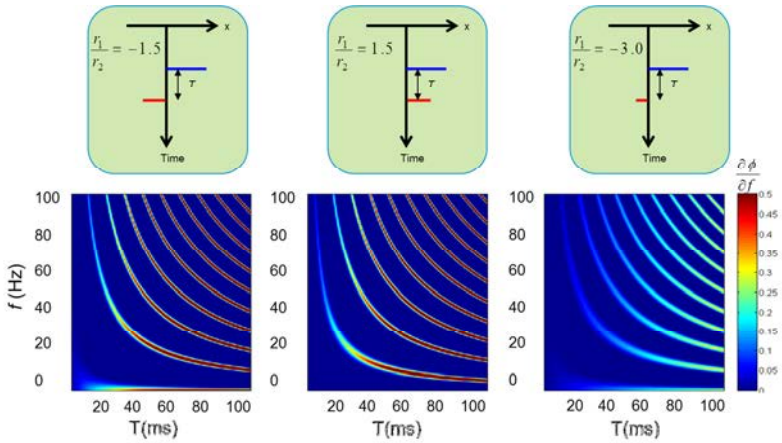

Figure 1 *Phase response of three different dipole reflectivity models as a function of thickness and frequency. Colour represents the derivative of phase with respect to frequency.*

of informative bandwidth of broadband seismic data is approaching ~2.0 Hz (JafarGandomi et al., 2015), which provides an overlap of two octaves with high-resolution velocity models. We propose to use this frequency overlap of velocity model and seismic data for low frequency phase estimation. The velocity may be obtained from high-definition tomography, interpolation of well-logs or a combination of both. It is worth mentioning that the method of velocity model estimation must be independent of the low-frequency phase of the seismic data.

Derivation of the phase correction operator

Starting with the noise-free convolutional model for seismic data (equation 2), we split the seismic spectrum into components below and above a certain cross-over frequency f_c:

$$A_S e^{i\phi_S} = \left(A_w e^{i\phi_w}.A_r e^{i\phi_r}\right)\Big|_0^{f_C} + \left(A_w e^{i\phi_w}.A_r e^{i\phi_r}\right)\Big|_{f_C}^{\infty}. \quad (3)$$

For brevity we drop the frequency dependency from the equation. We assume that we have an accurate low frequency impedance model. An approximation of reflectivity below f_c may be obtained from the background impedance model:

$$\tilde{A}_r e^{i\tilde{\phi}_r}\Big|_0^{f_C} = \frac{i\omega}{2} A_I e^{i\phi_I}\Big|_0^{f_C}, \quad (4)$$

where tilde indicates approximation and subscript I stands for impedance. Then a modelled seismic data can be synthesized below f_c using the estimated reflectivity (equation 4) and a zero-phase wavelet,

$$\tilde{A}_S e^{i\tilde{\phi}_S}\Big|_0^{f_C} = \left(A_w e^{i\phi_{w0}}.\tilde{A}_r e^{i\tilde{\phi}_r}\right)\Big|_0^{f_C} \leftarrow \phi_{w0} = 0.0. \quad (5)$$

Assuming $\tilde{A}_r = A_r$ below f_c, the low-frequency phase-correction operator $\chi(\omega)$ is decribed as,

$$\frac{e^{i\tilde{\phi}_S}}{e^{i\phi_S}}\Big|_0^{f_C} = e^{i\left[\tilde{\phi}_S - \phi_S\right]}\Big|_0^{f_C} = \chi(\omega)\Big|_0^{f_C}. \quad (6)$$

The phase-correction operator may then be used for quality control or applied to the seismic data to correct the low-frequency phase. The correction is a phase-only process and the amplitude response of the correction opertor is unity.

Synthetic example

We examine the performance of the proposed approach by applying it to a synthetic example. To generate the synthetic data with low-frequency phase error, we applied a frequency-dependent global phase rotation to a seismic stack from the North Sea. We use a global multi-layer tomography model

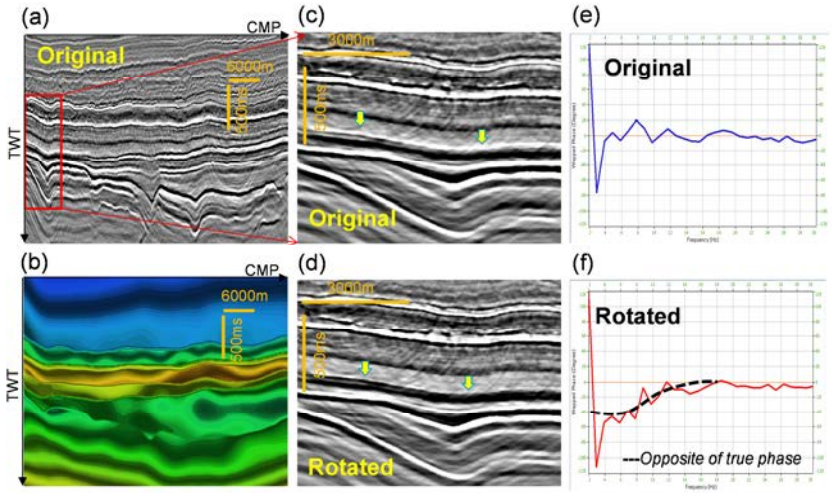

Figure2 *(a) Original seismic stack used to assess the performance of low-frequency phase estimation. (b) the velocity model used as an analogy for geology, (c) Zoomed original data, (d) low-frequency rotated data – zoomed, (e) phase correction operator in frequency domain for original data and (f) phase correction operator for rotated data.*

as the geological model, which contains a wide range of frequencies. Figure 2 shows the data, velocity model and corresponding phase-correction operators for original and rotated stacks. The estimated phase operator is obtained through matching all trace-pairs and averaging them within a three second time window where the velocity model has highest resolution. The operator matches very well with the opposite of the phase values applied to the rotated data, which confirms the robustness of the approach.

Real data example

We have applied the proposed low-frequency phase estimation method to a subset of a dense land broadband dataset recently acquired in the Sultanate of Oman. The data are processed through a broadband flow and depth migration, which gave a high quality broadband image. The velocity model was constructed using multi-layer travel-time tomography. Figure 3 depicts the good correlation between well-logs and tomography model for the velocity between 0-5 Hz.

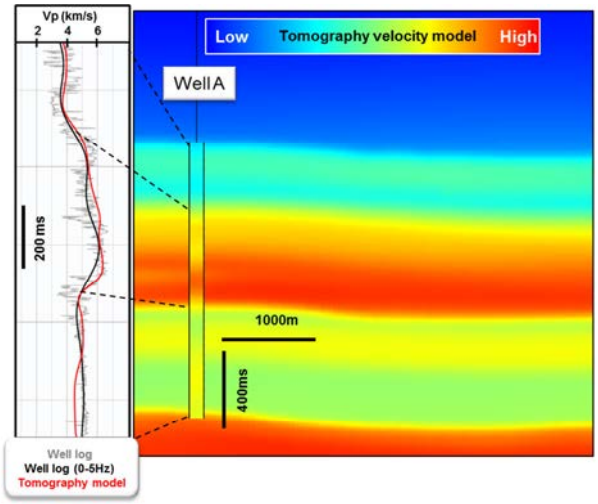

Figure 3 *Tomography velocity model used for low-frequency phase estimation along with QC with well-logs.*

The modelled seismic was obtained by convolving the reflectivity derived from the tomography model with a zero phase statistical wavelet extracted from the data. The phase correction operator (Figure 4) was obtained by matching the data to the modelled seismic within a 1.5 second time window and for all the frequencies. The phase correction was then applied to the data in the 0-5 Hz frequency range only, which is expected to contain the reliable information from the tomography model. Figure 5 shows the band-passed filtered 2-4 Hz stacks before and after phase correction. The data after phase correction has a better well-tie and better event definition. The arrows on the sections indicate a seismic negative phase event which is revealed after correction. In order to assess contribution of the corrected lower frequencies to the inversion we run a band-limited acoustic inversion on the data in the 2-60 Hz fequency range, with and without our phase correction, using a zero-phase wavelet. The inverted impedance after phase correction shows a better match with the well-logs (Figure 6). Furthermore away from the wells, the inversion artefacts caused by incorrect low-frequency phase are reduced resulting in an improved consistency of the layers. Also thin layers have been revealed. These observations are confirmed by controls at the well location as shown by the arrows on the figure. Similar observations are made at mutiple well locations.

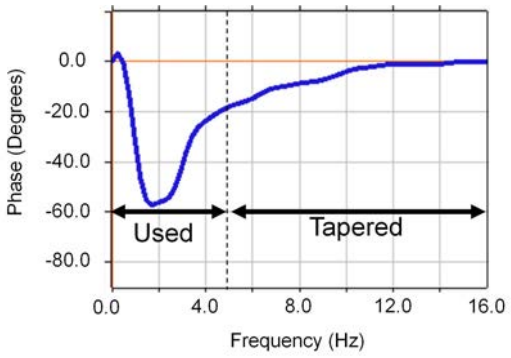

Figure 4 *Frequency response of low-frequency phase operator obtained from proposed velocity-driven approach.*

Conclusions

Separating geological tuning from wavelet phase is essential for accurate low-frequency phase estimation. We isolate the low-frequency phase of the wavelet in seismic data using travel-time tomography driven velocity models as an analogy for geology. We take advantage of the overlap in frequency range between broadband seismic and high-resolution tomography models to derive a low-

frequency phase correction operator. Our synthetic and real data examples verified with well-tie and inversion show the method to be reliable and robust.

Acknowledgments

We thank the Ministry of Oil and Gas of the Sultanate of Oman, PDO and CGG for permission to publish this work. We thank Gilles Lambaré for useful discussions.

References

Edgar, J.A. and Selvage, J.I. [2011]. Can thin beds be identified using statistical phase estimation?. First Break, 29(3), 55-65.

JafarGandomi, A., Hoeber, H., Coléou, T. and Mesdag, P. [2015] June. Assessing the Value of Low Frequencies in Seismic Inversion. In 77th EAGE Conference and Exhibition.

Longbottom, J., Walden, A.T. and White, R.E.[1988]. Principles and application of maximum kurtosis phase estimation. Geophysical Prospecting, 36(2), 115-138.

Schakel, M.D., and Mesdag, P.R. [2014]. Fully data-driven quantitative reservoir characterization by broadband seismic, SEG 84th Annual International Meeting, Expanded Abstract.

Vigée, L., Bader, M., Bénédini, A., Brillatz, C., Carotti, D., Cavalié, A., Coléou, T., Guillaume, P., Hénin, G., Lambaré, G. and Le Ruyet, T. [2014]. Tomographic Velocities-Challenges and Applications. In 76th EAGE Conference and Exhibition-Workshops.

Yang, F., Sablon, R. and Soubaras, R. [2016]. Ultra-low Frequency Phase Assessment for Broadband Data. In 78th EAGE Conference and Exhibition.

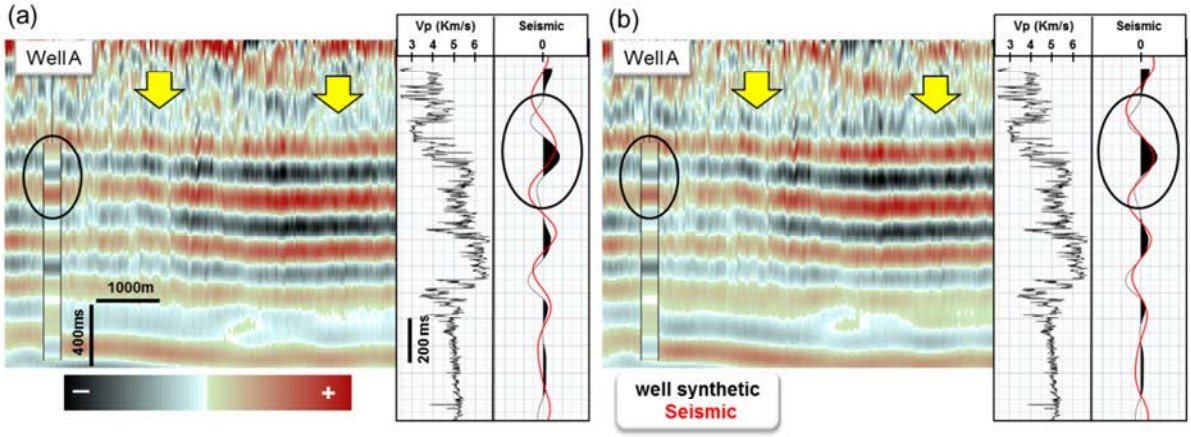

Figure 5 *Low-frequency band-passed data (2-4 Hz) (a) before and (b) after applying the phase-correction operator.*

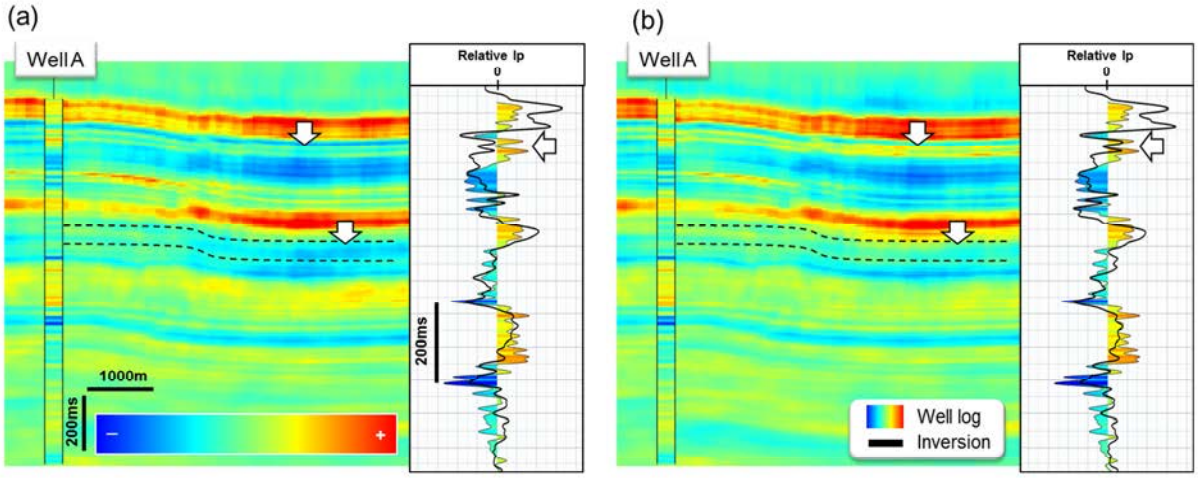

Figure 6 *Inverted relative impedances, (a) before and (b) after applying the low-frequency phase correction. The match to relative impedance from well data at four wells is shown below the inverted sections.*